OPTIMIZATION OF TOW-PLACED, TAILORED COMPOSITE LAMINATES

Adriana W. Blom*, Mostafa M. Abdalla* , Zafer Gürdal*
***Delft University of Technology, The Netherlands**

Keywords: *variable stiffness, tow placement, curved fibers, streamline, thickness, overlap*

Abstract

Fiber-reinforced composites are usually designed using constant fiber orientation in each ply. In certain cases, however, a varying fiber angle might be favorable for structural performance. This possibility can be fully utilized using tow placement technology. Because of the fiber angle variation, tow-placed courses may overlap and ply thickness will build up on the surface. This thickness build up affects manufacturing time, structural response, and surface quality of the finished product.

This paper will present a method for designing composite plates and shells using varying fiber angles. The thickness build-up is predicted as function of ply angle variation using a smeared approach. It is found that the thickness build-up is not unique and depends on the chosen start locations of fiber courses. Optimal fiber courses are formulated in terms of minimizing the maximum ply thickness, maximizing surface smoothness or combining these objectives, with and without periodic boundary conditions.

1 Introduction

In industry, fiber-reinforced composites are usually designed using a constant fiber orientation in each ply. The fiber angles in these laminates are typically 0, 90, and ±45 degrees. Traditionally the choice of these lay-ups was motivated by manufacturability, while nowadays lay-ups with changing or even non-conventional fiber angles are avoided because of the lack of allowables. However, research on composites with a varying in-plane fiber orientation has shown that variable stiffness can be beneficial for structural performance [1-11], because variable-stiffness laminates are able to redistribute the loading, as opposed to constant-stiffness laminates. In most cases curvilinear fiber paths manufactured by tow placement are used to construct the variable-stiffness laminates [4,5,8-10,12]. Jegley, Tatting and Gürdal [8-10] designed variable-stiffness flat plates with holes and demonstrated their effectiveness by building and testing several specimens.

Due to fiber angle variation, a tow-placed shell typically exhibits gaps and/or overlaps between adjacent courses and ply thickness will change along the surface [8-10,12]. The amount of gap/overlap affects structural response, manufacturing time, and surface quality of the finished product.

This paper presents a method for designing composite plates and shells using varying fiber angles. The thickness build-up is predicted as function of ply angle variation using a streamline analogy. It is found that the thickness build-up is not unique and depends on the chosen start locations of fiber courses. Optimal distributions of fiber courses are formulated in terms of minimizing the maximum ply thickness or maximizing surface smoothness, either with or without periodic boundary conditions. Subsequently the discrete thickness build-up resulting from the tow placement process will be shown as comparison to the smeared thickness approximation.

Finally, a number of applications for the developed methods and suggestions for future research will be given.

2 Streamline Analogy

For the construction of discrete fiber paths, a streamline analogy is being used. In this case

each streamline represents the centerline of a course, or if the course width is made infinitely small, each streamline will represent a single fiber. Mathematically a streamline is represented by a stream function

$$\Psi(x,y) = C \tag{1}$$

which connects all the points with a constant value C. For a given fiber angle variation $\theta(x,y)$, the streamlines can be found by solving the following partial differential equation:

$$\begin{aligned} \frac{d\Psi}{ds} &= \frac{\partial\Psi}{\partial x}\frac{dx}{ds} + \frac{\partial\Psi}{\partial y}\frac{dy}{ds} \\ &= \Psi_{,x}\cos\theta + \Psi_{,y}\sin\theta = 0 \end{aligned} \tag{2}$$

A unique solution for the stream function (and thus the location of the stream lines) depends on the boundary conditions. Before seeking a solution to the stream function, additional considerations relevant to the physical representation of the fiber paths are in order.

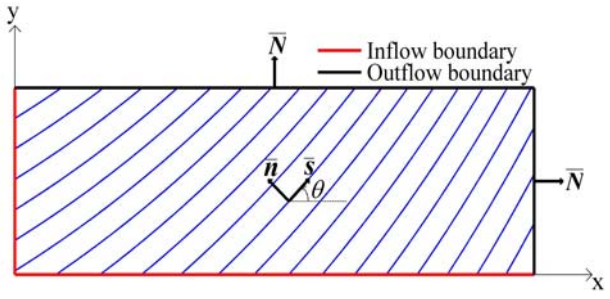

Fig. 1. Definitions

As stated earlier, the streamlines represent the central path of a finite width course. Unless the streamlines are parallel, the successive courses will always overlap each other when no gaps are allowed between them (or alternatively, the gaps will form between the passes if two successive finite width passes are not allowed to overlap). The amount of overlap depends on the distance between the course centerlines: when the distance is decreased the overlap area is increased. Although in reality these overlaps are discrete, a first approximation to the amount of overlap could be made by smearing out this discrete overlap to form a continuous thickness distribution. In this case, the smeared thickness, t, will be inversely proportional to the distance between adjacent courses, which can be explained as follows. If a number of N courses with a given width, w_c, and thickness has a fixed volume V, and if these successive courses are placed closer than the width of the courses, then the total width covered is less then $N \cdot w_c$, and the thickness has to be increased in order to maintain the same material volume V.

When the distance between two streamlines is $|dn|$, then $t \propto 1/|dn|$ (as explained above). Since $\Psi_{,n} = d\Psi/dn$ and $d\Psi$ between two streamlines is constant according to Eq. 1. the thickness t will be proportional to $\Psi_{,n}$ as follows:

$$t \propto \frac{1}{|dn|} = \frac{1}{\left(d\Psi/\Psi_{,n}\right)} = \frac{\Psi_{,n}}{d\Psi} \propto \Psi_{,n} \tag{3}$$

If $d\Psi$ is assumed to be 1, then $t = \Psi_{,n}$, which can be used to derive a direct correlation between the thickness distribution and the fiber angle variation:

$$-\bar{s}\bar{\nabla}(\ln t) = \bar{n}\bar{\nabla}\theta \tag{4}$$

in which $\bar{s}$ and $\bar{n}$ represent the tangent and normal vectors to a streamline, respectively, as shown in Fig. 1. The physical explanation of Eq. 4 is that the change in thickness along a streamline depends on the change of the fiber orientation perpendicular to that streamline. Since both vectors $\bar{s}$ and $\bar{n}$ depend on the given fiber angle distribution $\theta(x,y)$, the only unknown in Eq. 4 is the thickness. The thickness can now be determined by solving this equation, but since it is a differential equation boundary conditions are needed in order to obtain a unique solution. In accordance with streamline theory, boundary conditions are only needed at the inflow boundary, where the inflow boundary is defined by:

$$\bar{s} \cdot \bar{N} \leq 0 \qquad (5)$$

where $\bar{s}$ is the vector tangent to the streamline and $\bar{N}$ is the outward normal vector to the boundary, as shown in Fig. 1. By changing the thickness at the inflow boundary, the thickness distribution inside the domain and at the outflow boundaries will change.

3. Determining Boundary Conditions

There exist an infinite number of possible boundary conditions for which the thickness distribution associated with the streamlines can be found, but the most difficult part is to find the ones that are physically sensible for the problem in hand. In this paper the boundary conditions are established such that they fulfill a certain optimality criterion. The optimality criteria demonstrated in this paper are minimum maximum thickness, maximum smoothness, and combinations of these two. In addition to the optimality criterion, constraints such as a minimum of one or periodic boundary conditions can be enforced as well.

3.1 General Solution

By using the following change of variables: $\tau = \ln t$, Eq. 4 becomes:

$$-\bar{s}\bar{\nabla}\tau = \bar{n}\bar{\nabla}\theta \qquad (6)$$

Above equation is solved numerically by discretizing the derivatives, so that it is written as:

$$[M]\bar{\tau} = \bar{B} \qquad (7)$$

where $[M]$ is the matrix that represents the left hand side of Eq. 6, $\bar{\tau}$ is the vector that represents τ at every grid point and $\bar{B}$ is the vector that represents the right hand side of Eq. 6, as well as the boundary conditions. If the thickness at the inflow boundaries is assumed to be one everywhere ($\tau = 0$), a nominal solution can be found for $\bar{\tau}$, which will be referred to as $\bar{\tau}_0$. A general solution of Eq. 7 can be expressed as:

$$\bar{\tau} = \bar{\tau}_0 + [T]\bar{\tau}_{in} \qquad (8)$$

where each column j in matrix $[T]$ represents the influence of boundary grid point j on the thickness distribution in the complete domain, while satisfying Eq. 7. Since these columns are independent of each other and since Eq. 7 is a linear equation, any linear combination of these columns also represents a solution, as given by Eq. 8. The entries in $\bar{\tau}_{in}$ all render the thickness at a single point on the inflow boundary. By substituting Eq. 8 in Eq. 7, the thickness can be optimized for one of the criteria mentioned earlier by using $\bar{\tau}_{in}$ as design variables.

Often it is desired to have at least one layer of material everywhere so that no gaps exist. Therefore it is required that the thickness over the entire domain is at least one $(\bar{\tau} \geq \bar{0})$ in all optimizations described below.

3.2 Minimized Maximum Thickness

Minimizing the maximum thickness of the plate is the first optimality criterion that will be elaborated on in this paper. This criterion is relevant for judging how practical the resulting thickness distribution would be in a real life structure, as well as for determining if it is possible to manufacture a plate with constant thickness for the given fiber angle variation. If the thickness build-up is too severe (i.e. if one point is 100 or 1000 times thicker than another point) it will not be applicable to realistic structures.

In order to solve the min-max problem, the bound formulation as introduced by Olhoff [13] is used. This formulation introduces a new variable α, which represents the maximum thickness and which also serves as the new objective function for the minimization. Additionally, a constraint on the thickness at each grid point is being introduced, so that the thickness never exceeds the minimized maximum thickness, α:

$$\begin{aligned} & F_{\min} = \alpha \\ s.t. \quad & \tau_i \le \alpha \qquad i = 1,2,...,N_g \end{aligned} \tag{9}$$

where N_g is the number of grid points. The design variables that result from the optimization are substituted in Eq. 8 and then the thickness distribution is found by changing variables again: $t_i = e^{\tau_i}$.

3.3 Maximized Smoothness

Another possible optimization objective is to maximize the smoothness of the thickness distribution of the composite panel. Although in reality the change in thickness will always be discrete due to the discrete nature of tow courses, it would still be desirable for ply drops/overlaps to be distributed throughout the panel rather than to be concentrated at particular regions. In order to achieve this, smoothness is defined as the norm of the rate of change of thickness.

Smoothness is maximized by minimizing the H_1-norm of the thickness:

$$\min \qquad \tfrac{1}{2}\bar{\tau}^T[K]\bar{\tau} \tag{10}$$

where $[K]$ is the matrix that discretizes the Laplacian. Substituting the expression for $\bar{\tau}$ (Eq. 8) in Eq. 10 gives:

$$\begin{aligned} \tfrac{1}{2}\bar{\tau}^T[K]\bar{\tau} \quad = & \tfrac{1}{2}\bar{\tau}_0^T[K]\bar{\tau}_0 + \bar{\tau}_0^T[KT]\bar{\tau}_{in} \\ & + \tfrac{1}{2}\bar{\tau}_{in}^T[T]^T[K][T]\bar{\tau}_{in} \end{aligned} \tag{11}$$

The first term in this equation is constant, so that the objective function to be minimized is:

$$F_{\min} = \tfrac{1}{2}\bar{\tau}_{in}^T[K_r]\bar{\tau}_{in} - \bar{f}_r\bar{\tau}_{in} \tag{12}$$

with

$$\begin{aligned} [K_r] &= [T]^T[K][T] \\ \bar{f}_r &= -\bar{\tau}_0^T[K][T] \end{aligned} \tag{13}$$

The minimum of Eq. 12 can be found by differentiating it and equating it to zero, so that:

$$[K_r]\bar{\tau}_{in} = \bar{f}_r \tag{14}$$

This is a linear system that can be solved for $\bar{\tau}_{in}$. However, the $[K_r]$-matrix is one time singular and therefore one entry of $\bar{\tau}_{in}$ is given an assumed value so that the system can be solved. After the solution is substituted in Eq. 8, a constant can be added to $\bar{\tau}$ such that the condition of $\bar{\tau} \ge \bar{0}$ is being met (this will not change the H_1-norm, but will change the absolute value of thickness).

3.4 Combined Objective Function

Since both minimizing the maximum thickness and maximizing the smoothness are valid optimization criteria, designers might consider combining the two in order to obtain a better design. Depending on the designer, different weights can be assigned to the individual criteria. The objective functions of Eq. 9 and Eq. 12 can then be combined to form a new objective function:

$$F_{\min} = (1-w)\frac{\alpha}{\alpha^*} + w\frac{\tfrac{1}{2}\bar{\tau}_{in}^T[K_r]\bar{\tau}_{in} - \bar{f}_r\bar{\tau}_{in}}{\tfrac{1}{2}\bar{\tau}_{in}^{T^*}[K_r]\bar{\tau}_{in}^* - \bar{f}_r\bar{\tau}_{in}^*} \tag{15}$$

In this equation w is the weighing function that indicates the importance of the smoothness in the optimization. Furthermore the two objective functions are normalized by α^* and $\tfrac{1}{2}\bar{\tau}_{in}^{T^*}[K_r]\bar{\tau}_{in}^* - \bar{f}_r\bar{\tau}_{in}^*$, respectively, where α^* is the minimum maximum thickness obtained from Eq. 9 and $\bar{\tau}_{in}^*$ are the design variables for maximum smoothness as obtained by Eq. 12.

3.5 Periodic Boundary conditions

The present formulation would also be valid for cylindrical shells since points on a cylindrical surface are in one to one correspondence to points on a rectangular panel. Nevertheless, an important difference exists; in

the case of a cylindrical shell the solution must be periodic. When the ply angle variation is periodic, continuity in thickness is obtained by including the thickness periodicity constraints in the earlier described optimization routines. For periodicity in *y*-direction, this takes the form:

$$\tau(x_i,0) = \tau(x_i,b) \qquad 0 \le x_i \le l \qquad (16)$$

where l is the length and b is the width of the panel.

4. Discrete Fiber Courses

Once the smeared thickness distribution is obtained through one of the optimizations described above, the corresponding stream function can be obtained by integrating $\Psi_{,n}$ over dn:

$$\begin{aligned}\Psi(x,y) &= \int \Psi_{,n}\, dn \\ &= \int \frac{d\Psi}{dx}\frac{dx}{dn}dn + \int \frac{d\Psi}{dy}\frac{dy}{dn}dn \\ &= \int \Psi_{,x}dx + \int \Psi_{,y}dy\end{aligned} \qquad (17)$$

The derivatives of Ψ with respect to x and y can be expressed as functions of $\Psi_{,s}$ and $\Psi_{,n}$ as follows:

$$\begin{aligned}\Psi_{,x} &= \Psi_{,s}\cdot\cos\theta - \Psi_{,n}\sin\theta \\ \Psi_{,y} &= \Psi_{,s}\cdot\sin\theta + \Psi_{,n}\cos\theta\end{aligned} \qquad (18)$$

Since $\Psi_{,s} = 0$ and $\Psi_{,n} = t$, the combination of Eqs. 18 and 19 will give:

$$\begin{aligned}\Psi(x,y) = &-\int_0^x t(x,y)\sin\theta(x,y)dx \\ &+\int_0^y t(x,y)\cos\theta(x,y)dy\end{aligned} \qquad (19)$$

Both $t(x,y)$ and $\theta(x,y)$ are known functions, so that $\Psi(x,y)$ can be solved. By plotting the contour lines of this function at fixed values $d\Psi$ from each other, the streamlines are found that could represent the centerlines of the actual fiber courses. The constant of integration will determine the exact location of the fiber courses, which can be used for staggering in case of multiple plies with the same fiber angle distribution. Once the course centerlines are known, discrete courses can be placed on top of them and the discrete thickness distributions can be found.

5. Results

To illustrate the differences between the various optimality criteria described in section 3, an example panel is analyzed which has the following linear angle variation in x-direction:

$$\theta(x,y) = -30 - 30\frac{x}{l} \qquad (20)$$

such that the fiber orientation is at -30 degrees at the left side of the panel ($x = 0$) and -60 degrees at the right side of the panel ($x = l$). The length to width ratio of the panels is 3.

Fig. 2a. shows the thickness distribution of a panel for which the maximum thickness is minimized. The thickness along the left and top edge is one, which means that there are no overlaps on these sides. The maximum thickness occurs in the lower right corner of the panel. The thickness distribution of a panel with maximized smoothness is presented in Fig. 2b. Compared to the first panel the maximum thickness is increased by approximately 20 percent, while smoothness is improved by 40 percent. In Fig. 2c. the smeared thickness for the combined objective with $w = 0.5$ is plotted. Since both maximum thickness and smoothness are included in the objective function, the increase in maximum thickness is only 7 percent, while the improvement in smoothness is 30 percent when compared to the first panel. Finally a panel with periodic boundary conditions is shown in Fig. 2d. The maximum thickness of this panel is more than 40 percent larger than the minimum maximum thickness, and also smoothness is decreased.

The discrete thickness distributions corresponding to the four smeared thickness distributions of Fig. 2. are shown in Fig. 3. The width of these courses was assumed to be 1/6 of

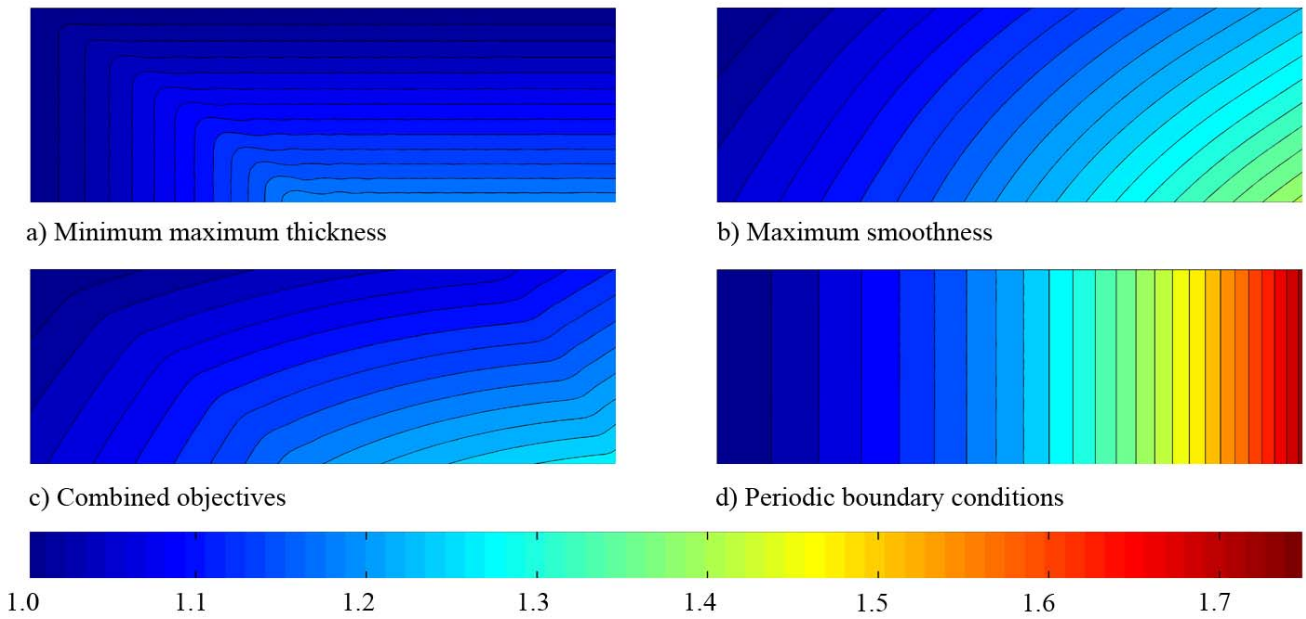

Fig. 2. Thickness distribution for various optimization criteria

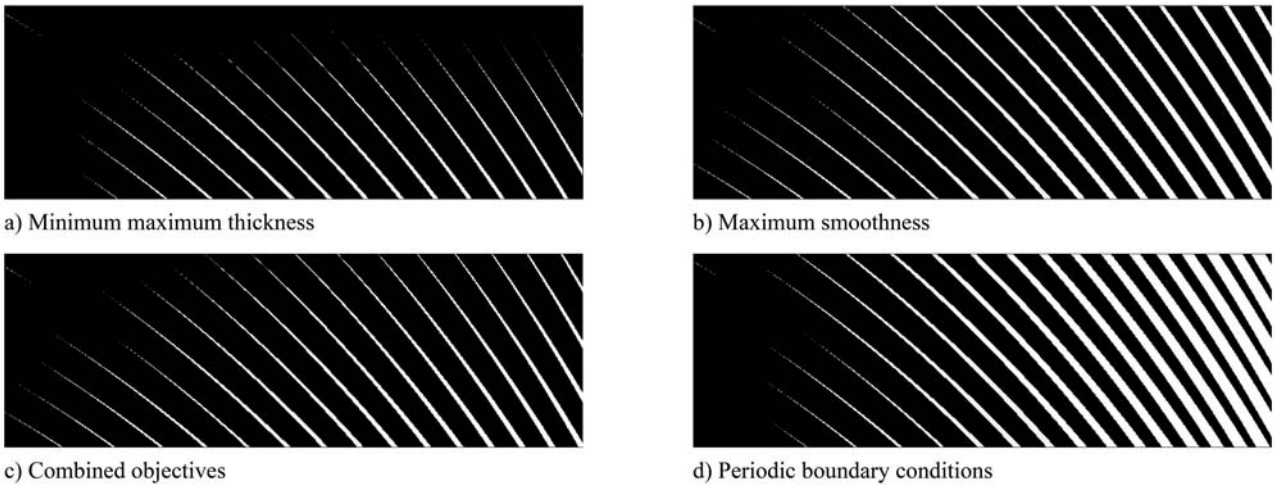

Fig. 3. Discrete thickness build-up (black = 1 layer, white = 2 layers)

the panel width. Fig. 3a. clearly shows the least amount of overlap. If a laminate with constant thickness was desired, the fiber paths obtained by this optimization can be used as basic paths and the overlaps could be eliminated by cutting individual tows on the sides of the courses. The smoothness of the laminate in Fig. 3b. is not very apparent, until multiple plies are stacked on top of each other and staggered with respect to each other. The combined objective laminate of Fig. 3c. is indeed in between the laminates of Fig. 3a. and Fig. 3b. Finally, the relatively large thickness build-up of the laminate with periodic boundary conditions is translated in large overlap areas, as shown in Fig. 3d.

6. Future Research

In this paper it was successfully demonstrated that a stream line analogy can be used to predict and influence the thickness distribution in a laminate with variable fiber angles. Different objectives for optimization

were considered, and in the future others, such as minimum volume, might be explored as well.

In addition to one-ply designs, the developed methods could be used to design complete laminates with both varying fiber angles and varying thickness. One approach would be to design the laminate using lamination parameters and thickness [6,7,14] as spatially varying design variables, and then as a post-processing step, multiple plies with varying fiber angles and their corresponding thickness distributions could be fit in order to match both the desired lamination parameters and thickness distribution as close as possible.

Finally, a similar method will be developed for curved surfaces in order to expand the applicability of the method.

References

[1] Hyer M.W. and Charette R.F. "The use of curvilinear fiber format in composite structure design". *Proceedings of the 30th AIAA/ASME/ASCE/AHS/ASC Structures, Structural Dynamics and Materials (SDM) Conference*, New York, NY, paper no. 1404, 1989.

[2] Hyer M.W. and Lee H.H. "The use of curvilinear fiber format to improve buckling resistance of composite plates with central holes". *Composite Structures*, Vol. 18, pp 239-261, 1991.

[3] Nagendra S., Kodiyalam A., Davis J.E. and Parthasarathy V.N. "Optimization of tow fiber paths for composite design". *Proceedings of the 36th AIAA/ASME/ASCE/AHS/ASC Structures, Structural Dynamics and Materials (SDM) Conference*, New Orleans, LA, paper no. 1275, 1995.

[4] Waldhart C.J. and Gürdal Z. "Analysis of tow placed, parallel fiber, variable stiffness laminates". *Proceedings of the 37th AIAA/ASME/ASCE/AHS/ASC Structures, Structural Dynamics and Materials (SDM) Conference*, Salt Lake City, UT, paper no. 1569, 1996.

[5] Parnas L., Oral S. and Ceyhan U. "Optimum design of composite structures with curved fiber courses". *Composite Science and Technology*, Vol. 63, pp 1071-1082, 2003.

[6] Setoodeh S., Abdalla M.M. and Gürdal Z. "Design of variable stiffness laminates using lamination parameters". *Composites, Part B: Engineering*, Vol. 37, pp 301-309, 2006.

[7] Abdalla M.M., Setoodeh S. and Gürdal Z. "Design of variable stiffness composite panels for maximum fundamental frequency using lamination parameters". *Proceedings of the European Conference on Spacecraft Structures, Materials and Mechanical Testing*, Noordwijk, The Netherlands, 2005.

[8] Tatting B.F. and Gürdal Z. "Design and manufacturing of elastically tailored tow-placed plates". *NASA/CR-2002-211919*.

[9] Tatting B.F. and Gürdal Z. "Automated finite element analysis of elastically-tailored plates". *NASA/CR-2003-212679*.

[10] Jegley D.C., Tatting B.F. and Gürdal Z. "Tow-steered panels with holes subjected to compression or shear loading". *Proceedings of the 36th AIAA/ASME/ASCE/AHS/ASC Structures, Structural Dynamics and Materials (SDM) Conference*, Austin, TX, paper no. 2081, 2005.

[11] Blom A.W., Setoodeh S., Hol J.M.A.M. and Gürdal Z. "Design of variable-stiffness conical shells for maximum fundamental frequency". *Proceedings of the 3rdEuropean Conference on Computational Mechanics: Solids, Structures and Coupled Problems in Engineering*, Lisbon, Portugal, June 2006.

[12] Blom A.W., Tatting B.F., Hol J.M.A.M. and Gürdal Z. "Path definitions for elastically tailored conical shells". *Proceedings of the 47th AIAA/ASME/ASCE/AHS/ASC Structures, Structural Dynamics and Materials (SDM) Conference*, Newport, RI, paper no. 1940, 2006.

[13] Olhoff N. "Multicriterion structural optimization via bound formulation and mathematical programming". *Structural Optimization*, Vol 1, pp 11-17, 1989.

[14] Setoodeh S., Blom A.W., Abdalla M.M. and Gürdal Z. "Generating curvilinear fiber paths from lamination parameters distribution". *Proceedings of the 47th AIAA/ASME/ASCE/AHS/ASC Structures, Structural Dynamics and Materials (SDM) Conference*, Newport, RI, paper no. 1875, 2006.

Appendix A

The derivatives of the stream function are:

$$\Psi_{,x} = -\Psi_{,n}\sin\theta = -t\sin\theta$$
$$\Psi_{,y} = \Psi_{,n}\cos\theta = t\cos\theta$$

The second derivatives of the stream function are:

$$\Psi_{,xy} = -t\cos\theta\cdot\theta_{,y} - \sin\theta\cdot t_{,y}$$
$$\Psi_{,yx} = -t\sin\theta\cdot\theta_{,x} + \cos\theta\cdot t_{,x}$$

Continuity of the second derivatives of the stream function implies that $\Psi_{,xy} = \Psi_{,yx}$ so that:

$$\begin{aligned}\Psi_{,xy} - \Psi_{,yx} &= -t \cdot \left(\cos\theta \cdot \theta_{,y} - \sin\theta \cdot \theta_{,x}\right) \\ &\quad -\left(\sin\theta \cdot t_{,x} + \cos\theta \cdot t_{,x}\right) \\ &= 0\end{aligned}$$

Rearrangement gives:

$$-\left(\cos\theta \frac{t_{,x}}{t} + \sin\theta \frac{t_{,y}}{t}\right) = -\sin\theta \cdot \theta_{,x} + \cos\theta \cdot \theta_{,y} \qquad \text{(A)}$$

Using the following definitions:

$$\bar{n} = \begin{Bmatrix} -\sin\theta \\ \cos\theta \end{Bmatrix} \qquad \bar{\nabla}\theta = \begin{Bmatrix} \theta_{,x} \\ \theta_{,y} \end{Bmatrix}$$

$$\bar{s} = \begin{Bmatrix} \cos\theta \\ \sin\theta \end{Bmatrix} \qquad \bar{\nabla}(\ln t) = \begin{Bmatrix} t_{,x}/t \\ t_{,y}/t \end{Bmatrix}$$

Eq. A can be written as:

$$-\bar{s}\bar{\nabla}(\ln t) = \bar{n}\bar{\nabla}\theta$$